



Epitaxial growth of the first five members of the $\text{Sr}_{n+1}\text{Ti}_n\text{O}_{3n+1}$ Ruddlesden–Popper homologous series

J. H. Haeni, C. D. Theis, D. G. Schlom, W. Tian, X. Q. Pan, H. Chang, I. Takeuchi, and X.-D. Xiang

Citation: *Applied Physics Letters* **78**, 3292 (2001); doi: 10.1063/1.1371788

View online: <http://dx.doi.org/10.1063/1.1371788>

View Table of Contents: <http://scitation.aip.org/content/aip/journal/apl/78/21?ver=pdfcov>

Published by the [AIP Publishing](#)

Articles you may be interested in

Growth, characterization, and uniformity analysis of 200 mm wafer-scale SrTiO_3/Si

J. Vac. Sci. Technol. B **28**, C3A12 (2010); 10.1116/1.3292509

Epitaxial growth and magnetic properties of the first five members of the layered $\text{Sr}_{n+1}\text{Ru}_n\text{O}_{3n+1}$ oxide series

Appl. Phys. Lett. **90**, 022507 (2007); 10.1063/1.2430941

Growth of biaxially textured $\text{Ba}_x\text{Pb}_{1-x}\text{TiO}_3$ ferroelectric thin films on amorphous Si_3N_4

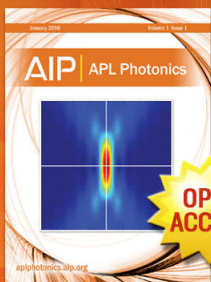
J. Appl. Phys. **97**, 034103 (2005); 10.1063/1.1806994

Thickness and oxygen pressure dependent structural characteristics of BaTiO_3 thin films grown by laser molecular beam epitaxy

J. Appl. Phys. **87**, 7442 (2000); 10.1063/1.373007

BaTiO_3 thin films grown on SrTiO_3 substrates by a molecular-beam-epitaxy method using oxygen radicals

J. Appl. Phys. **81**, 693 (1997); 10.1063/1.364209



Launching in 2016!

The future of applied photonics research is here

AIP | **APL Photonics**

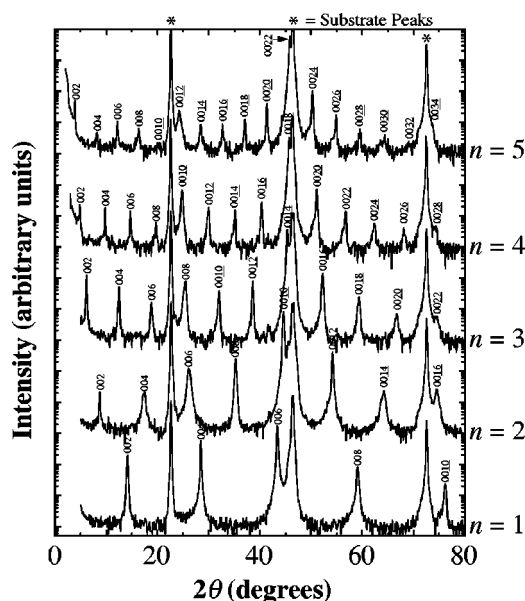


FIG. 2. θ - 2θ x-ray diffraction scans of the first five members of the $\text{Sr}_{n+1}\text{Ti}_n\text{O}_{3n+1}$ Ruddlesden-Popper homologous series grown on SrTiO_3 (001) substrates. Substrate peaks are labeled with a (*), and the plots are offset for clarity. The narrow peaks at the correct 2θ positions indicate that each of the films is single phase.

which are metastable. For example, McCoy *et al.*¹⁶ concluded that $\text{Sr}_3\text{Ti}_2\text{O}_7$ and SrTiO_3 are the only stable $\text{Sr}_{n+1}\text{Ti}_n\text{O}_{3n+1}$ phases, whereas Noguera¹⁷ concluded that Sr_2TiO_4 , $\text{Sr}_3\text{Ti}_2\text{O}_7$, and SrTiO_3 are the only stable phases.

We have used MBE to overcome these challenging barriers to the synthesis of these materials. Each of the unit cells of this series is made up of different sequences of SrO and TiO_2 layers (Fig. 1). SrTiO_3 has the perovskite crystal structure with alternating TiO_2 and SrO layers; we refer to the combination of these two layers as a perovskite sheet. The $n=1$ (Sr_2TiO_4) compound has an additional SrO layer (making a double SrO layer) disrupting each perovskite sheet along the c axis. Subsequent members of the series have an increasing number of perovskite sheets separated by the double SrO layers. By changing the shuttering sequence of Sr and Ti ions to match the layering sequence of the desired phase, we have grown epitaxial films of these phases despite the fact that they melt incongruently, have structural transitions, and lack sufficient driving forces for formation.

The $n=1-5$ members of this series were grown using an oxide MBE system. Before growth, the substrates were etched with a buffered HF solution to achieve a TiO_2 -terminated surface.¹⁸ Monolayer doses (6.6×10^{14} atoms/cm²) of Sr and Ti were deposited in a sequential manner on well oriented ($\pm 0.1^\circ$) SrTiO_3 (001) substrates. For the double-SrO layers in these structures, a dose corresponding to twice the monolayer dose was delivered. The average flux of both the Sr and Ti sources was 1.0×10^{14} atoms/cm²·s for all growths. During growth, the substrate temperature was 750 °C as measured by an optical pyrometer. The substrate was immersed in a continuous flux of molecular oxygen, yielding a background pressure of 2×10^{-7} Torr. The thicknesses of the films were 470, 410, 565, 540, and 590 Å, for the $n=1-5$ films, respectively.

A combination of reflection high-energy electron diffraction (RHEED) intensity oscillations and atomic absorption spectroscopy (AA) was used to adjust the stoichiometry of the Sr and Ti molecular beams and ensure that a complete monolayer of each cation was deposited in each shuttered cycle.¹⁹ A series of growths revealed that the phase-pure synthesis of these compounds required that both the stoichiometry and absolute monolayer doses not be off by more than about 1%.

Films grown outside this narrow composition window (i.e., where the stoichiometry or absolute monolayer doses are off by more than 1%) show clear evidence of intergrowths within the desired phase when examined by x-ray diffraction. A nonperiodic stacking sequence in the c direction (intergrowths) causes certain x-ray peaks to split, broaden, or shift in 2θ .^{20,21} The monolayer-by-monolayer deposition of films with the correct stoichiometry resulted in single-phase films whose x-ray peaks show narrow widths and the correct 2θ positions (Fig. 2). The c -axis lattice constant of these phases as determined by a Nelson-Riley²² analysis of the diffraction peak positions is 12.46 ± 0.02 Å, 20.35 ± 0.05 Å, 28.1 ± 0.2 Å, 35.6 ± 0.2 Å, and 43.5 ± 1.0 Å for the $n=1-5$ phases, respectively. This compares to the bulk reported lattice constants of 12.601, 20.38, and 28.1 Å for the $n=1-3$ phases, respectively.⁷ X-ray ϕ scans of the 103, 105, 107, 109 and 1011 peaks of the $n=1-5$ films, respectively, indicated epitaxial, c -axis films with orientation $(001)\text{Sr}_{n+1}\text{Ti}_n\text{O}_{3n+1} \parallel (001)\text{SrTiO}_3$ and $[100]\text{Sr}_{n+1}\text{Ti}_n\text{O}_{3n+1} \parallel [100]\text{SrTiO}_3$.²³ The in-plane lat-

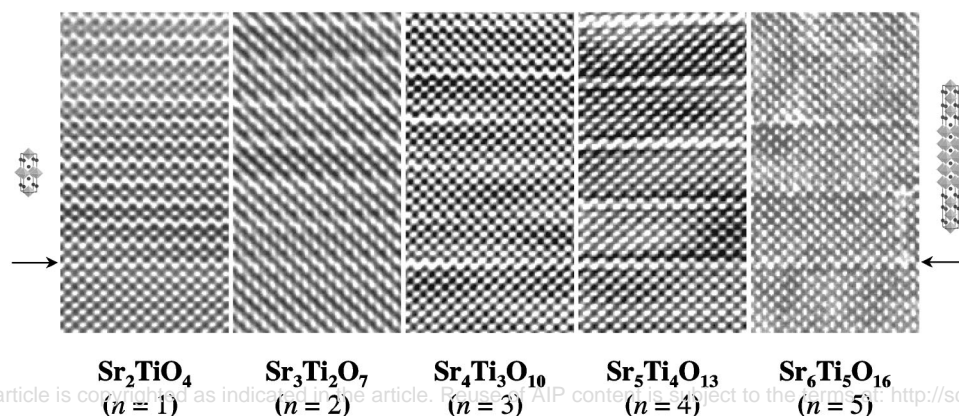


FIG. 3. Cross-sectional HRTEM images (from left to right) of the $n=1$ (Sr_2TiO_4), $n=2$ ($\text{Sr}_3\text{Ti}_2\text{O}_7$), $n=3$ ($\text{Sr}_4\text{Ti}_3\text{O}_{10}$), $n=4$ ($\text{Sr}_5\text{Ti}_4\text{O}_{13}$), and $n=5$ ($\text{Sr}_6\text{Ti}_5\text{O}_{16}$) films. A model of the crystal structure of the $n=1$ and $n=5$ members are adjacent to the corresponding images showing the position of the SrO double layers and perovskite layers. The arrows mark the position of the interface of the films with the homoepitaxial SrTiO_3 buffer layer.

tice constants determined from the x-ray measurements ranged from $3.83 \pm 0.05 \text{ \AA}$ to $3.94 \pm 0.05 \text{ \AA}$.²³

A JEOL 4000EX high-resolution transmission electron microscope (HRTEM) operated at 400 kV was used to examine the local nanostructure of these films.²³ Figure 3 is a cross-sectional HRTEM image showing the interface of each of these phases with the SrTiO₃ homoepitaxial buffer layer. Equal spacing between the double SrO layers (light lines) indicates a single-phase film. All of the imaged areas of the $n = 1 - 3$ films look similar to the region shown in Fig. 3 with no intergrown regions observed. However, some intergrowths of higher n phases were observed in localized regions of the $n = 4$ and 5 films. In addition, defects consisting of vertical SrO double layers (see Fig. 3) were commonly seen adjacent to an intergrowth.²³ Such vertically running SrO double layers have also been seen in bulk Sr_{*n*+1}Ti_{*n*}O_{3*n*+1} samples and have been shown to have low-energy interfaces.¹⁶ They have also been observed in other perovskite homologous series.^{20,24-26} The intergrowths in these samples are most likely the result of slight monolayer-to-monolayer composition fluctuations during the deposition of the films. These (<1%) fluctuations are present in all of the growths, but the higher n phases seem to be more sensitive to them, as manifested by the more frequent intergrowths. We believe that theoretically there is no limit to the n value of these Sr_{*n*+1}Ti_{*n*}O_{3*n*+1} phases that can be synthesized with MBE. In reality, we are limited by the composition control limits of the AA system and RHEED technique. An attempt to synthesize the $n = 10$ phase resulted in an x-ray diffraction pattern with some diminished and broadened peaks, indicating significant intergrowths.²¹

The growth of epitaxial films allowed the ϵ_{33} dielectric constant tensor coefficient to be measured in these anisotropic materials. Previous measurements of polycrystalline Sr₂TiO₄ and Sr₃Ti₂O₇ samples reported the average dielectric constant (ϵ_r) to be 38 and 50, respectively.¹¹ Room temperature dielectric measurements were made on the $n = 1, 2$, and ∞ members of this series with a scanning evanescent microwave microscope (SEMM)^{27,28} at 1 GHz and in a parallel plate capacitor structure with an HP 4284A at 1 kHz. The films measured with the SEMM were 1000 Å thick and grown directly on a (001)LaAlO₃-Sr₂AlTaO₆ (LSAT) substrate. LSAT (cubic, $a = 7.737 \text{ \AA}$)²⁹ has an excellent lattice match with these phases and was used instead of SrTiO₃ because its low dielectric constant ($\epsilon_r = 22.5$)³⁰ did not interfere with the measurement. The capacitor structures consist of an MBE-grown 1000 Å Sr_{0.85}La_{0.15}TiO₃ bottom electrode, a 1000 Å Sr_{*n*+1}Ti_{*n*}O_{3*n*+1} film, and 0.3 mm diameter Cr/Au top electrodes.

Both of these techniques show excellent agreement for the values of ϵ_{33} . The first member of this series, Sr₂TiO₄, has a dielectric constant tensor coefficient ϵ_{33} of 44 ± 4 , while Sr₃Ti₂O₇ has an ϵ_{33} of 86 ± 6 . The dielectric loss ($\tan \delta$) of all films measured was lower than the detection limit of the SEMM (i.e., less than 1.5%). The magnitude of ϵ_{33} makes these low n Sr_{*n*+1}Ti_{*n*}O_{3*n*+1} phases not only of interest for tunable dielectric devices, but also for alternative gate oxides in MOSFETs. Sr₂TiO₄ has several potential ad-

vantages over SrTiO₃ in this application including its 38% better lattice match with Si, higher band gap¹⁷ (to reduce leakage), lower thermodynamic driving force for reaction with Si, and greater stability against reduction.

The authors gratefully acknowledge the support of the Department of Energy under Grant No. DE-FG02-97ER45638 for the development of the thin film growth technique and structural characterization, and support by DARPA through Contract No. DABT63-98-1-002 for the analysis of the dielectric properties of these materials.

- ¹A. Brazdeikis, A. Vailionis, and A. S. Flodstrom, *Physica C* **235-240**, 711 (1994).
- ²D. G. Schlom, J. N. Eckstein, I. Bozovic, Z. J. Chen, A. F. Marshall, K. E. von Dessenoneck, and J. S. Harris, Jr., *Proc. SPIE* **1285**, 234 (1990).
- ³M. E. Klausmeier-Brown, G. F. Virshup, I. Bozovic, and J. N. Eckstein, *Appl. Phys. Lett.* **60**, 2806 (1992).
- ⁴R. Ramesh, S. Jin, and P. Marsh, *Nature (London)* **346**, 420 (1990).
- ⁵A. Schilling, M. Cantoni, J. D. Guo, and H. R. Ott, *Nature (London)* **363**, 56 (1993).
- ⁶R. J. D. Tilley, *J. Solid State Chem.* **21**, 293 (1977).
- ⁷S. N. Ruddlesden and P. Popper, *Acta Crystallogr.* **10**, 538 (1957); **11**, 54 (1958).
- ⁸F. W. Van Keuls, R. R. Romanofsky, D. Y. Bohman, M. D. Winters, and F. A. Miranda, *Appl. Phys. Lett.* **71**, 3075 (1997).
- ⁹X. X. Xi, H.-C. Li, W. Si, A. A. Sirenko, I. A. Akimov, J. R. Fox, A. M. Clark, and J. Hao, *J. Electroceram.* **4**, 393 (2000).
- ¹⁰R. A. McKee, F. J. Walker, and M. F. Chisholm, *Phys. Rev. Lett.* **81**, 3014 (1998).
- ¹¹W. Kwestroo and H. A. M. Paping, *J. Am. Ceram. Soc.* **42**, 292 (1959).
- ¹²T. Nakamura, P.-H. Sun, Y. J. Shan, Y. Inaguma, M. Itoh, I.-S. Kim, J.-H. Sohn, M. Ikeda, T. Kitamura, and H. Konagaya, *Ferroelectrics* **196**, 205 (1997).
- ¹³*Phase Diagrams for Ceramists 1969 Supplement*, edited by E. M. Levin, C. R. Robbins, and H. F. McMurdie (American Ceramic Society, Columbus, 1969), p. 93.
- ¹⁴G. J. McCarthy, W. B. White, and R. Roy, *J. Am. Ceram. Soc.* **52**, 463 (1969).
- ¹⁵K. R. Udayakumar and A. N. Cormack, *J. Am. Ceram. Soc.* **71**, C-469 (1988).
- ¹⁶M. A. McCoy, R. W. Grimes, and W. E. Lee, *Philos. Mag.* **A 75**, 833 (1997).
- ¹⁷C. Noguera, *Philos. Mag. Lett.* **80**, 173 (2000).
- ¹⁸M. Kawasaki, K. Takahashi, T. Maeda, R. Tsuchiya, M. Shinohara, O. Ishiyama, T. Yonezawa, M. Yoshimoto, and H. Koinuma, *Science* **266**, 1540 (1994).
- ¹⁹J. H. Haeni, C. D. Theis, and D. G. Schlom, *J. Electroceram.* **4**, 385 (2000).
- ²⁰R. Seshadri, M. Hervieu, C. Martin, A. Maignan, B. Domenges, B. Raveau, and A. N. Fitch, *Chem. Mater.* **9**, 1778 (1997).
- ²¹S. Hendricks and E. Teller, *J. Chem. Phys.* **10**, 147 (1942).
- ²²J. B. Nelson and D. P. Riley, *Proc. Phys. Soc. London* **57**, 160 (1945).
- ²³W. Tian, X. Q. Pan, J. H. Haeni, and D. G. Schlom, *J. Mater. Res.* (to be published).
- ²⁴K. Hawkins and T. J. White, *Philos. Trans. R. Soc. London, Ser. A* **336**, 541 (1991).
- ²⁵T. Williams, F. Lichtenberg, A. Reller, and G. Bednorz, *Mater. Res. Bull.* **26**, 763 (1991).
- ²⁶J. Sloan, P. D. Battle, M. A. Green, M. J. Rosseinsky, and J. F. Vente, *J. Solid State Chem.* **138**, 135 (1998).
- ²⁷C. Gao and X.-D. Xiang, *Rev. Sci. Instrum.* **69**, 3846 (1998).
- ²⁸H. Chang, I. Takeuchi, and X.-D. Xiang, *Appl. Phys. Lett.* **74**, 1165 (1999).
- ²⁹D. Mateika, H. Kohler, H. Laudan, and E. Volkel, *J. Cryst. Growth* **109**, 447 (1991).
- ³⁰S. C. Tidrow, A. Tauber, W. D. Wilber, R. T. Lareau, C. D. Brandle, G. W. Berkstresser, A. J. Ven Graitis, D. M. Potrepka, J. I. Budnick, and J. Z. Wu, *IEEE Trans. Appl. Supercond.* **17**, 1766 (1997).